Supplementary Information

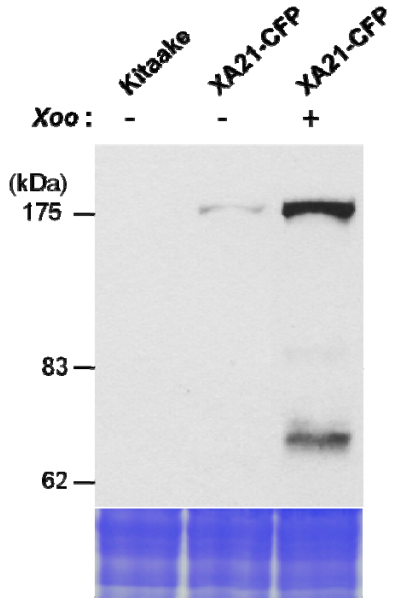

Supplementary Figure S1. Immunodetection of full-length XA21 and the XA21 C-terminal cleavage product.

Total protein extracted from Kitaake wild type and rice plants carrying a C-terminal cyan fluorescent protein (CFP)-tagged XA21 under control of its native promoter (XA21-CFP, T_2, 15A-1-7) before (-) and 18 hours after (+) *Xoo* inoculation. Equal amounts (150 µg) of protein were analyzed by 8% SDS-PAGE and immunobloted with anti-GFP antibody. Equal loading of total proteins was confirmed by Coomassie blue staining of proteins (lower panel).

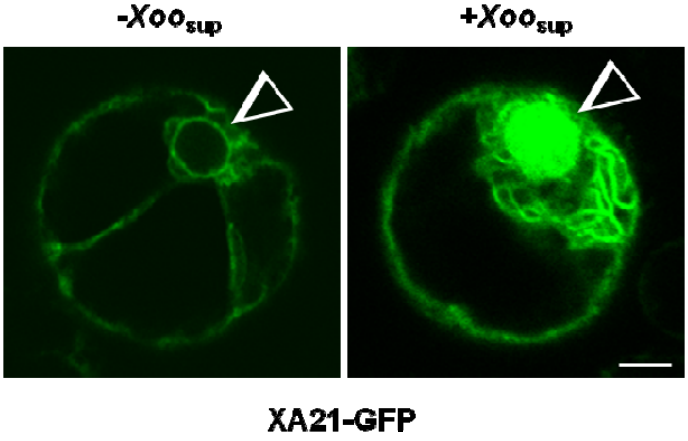

Supplementary Figure S2. Nuclear translocation of XA21-GFP in protoplasts after treatment of *Xoo* supernatant (+*Xoo*$_{sup}$).

Ubi-XA21-GFP was introduced into rice protoplast cells by PEG-mediated transformation. Supernatant of *Xoo* was applied 16 hours after transformation and the expression of the introduced genes was observed one hour after supernatant treatment (+*Xoo*$_{sup}$). Images were collected with a Leica True Confocal Scanner SPE confocal microscope and coded in green for GFP. Arrow heads mark the nuclei. Scale bar, 10 μm.

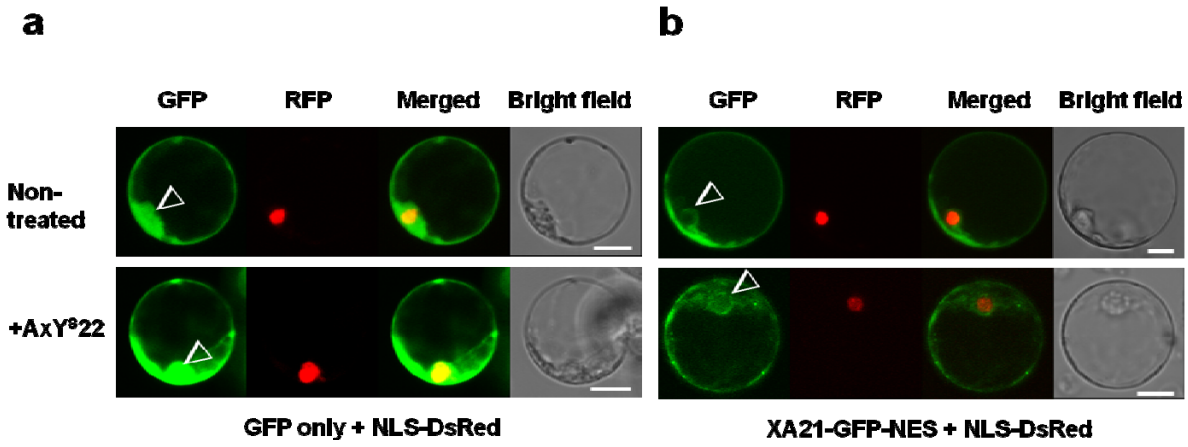

Supplementary Figure S3. Addition of a nuclear export signal (NES) inhibits nuclear accumulation of XA21-GFP without interfering with plasma membrane localization.

Ubi-GFP (a) and C-terminal NES tagged XA21-GFP under the control of *Ubi* promoter (*Ubi-Xa21-GFP-NES*) (b) were introduced into rice protoplast cells by PEG-mediated transformation. *NLS-DsRed* was co-transformed for a nucleus marker. The expression of the introduced genes was observed 16 hours after transformations. Images were collected with a Leica True Confocal Scanner SPE confocal microscope and coded in green and red for GFP and DsRed, respectively. Arrow heads mark the nuclei. Scale bar, 10 μm.

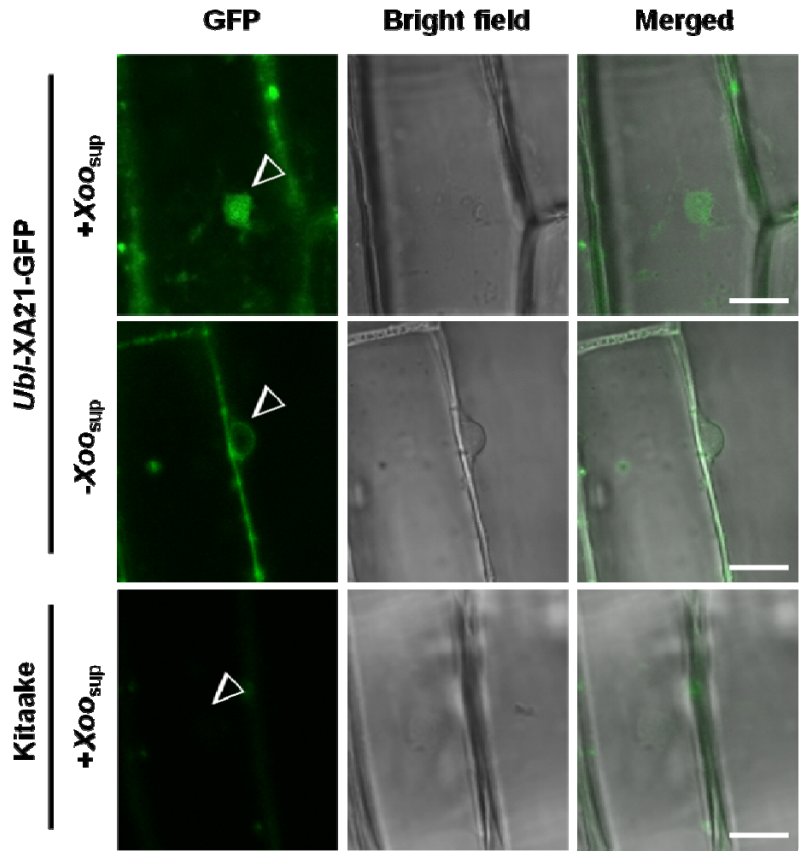

Supplementary Figure S4. Nuclear translocation of XA21-GFP in protoplasts after treatment of *Xoo* supernatant (+Xoo_{sup}).

In planta translocation of XA21-GFP in *Ubi*-XA21-GFP and Kitaake wild type plants was determined using confocal microscopy. Intact adaxial sheath epidermal cells were observed one hour after supernatant treatment (+Xoo_{sup}). Images were collected with a Leica True Confocal Scanner SPE confocal microscope and coded in green for GFP. Arrow heads mark the nuclei. Scale bar, 10 μm.

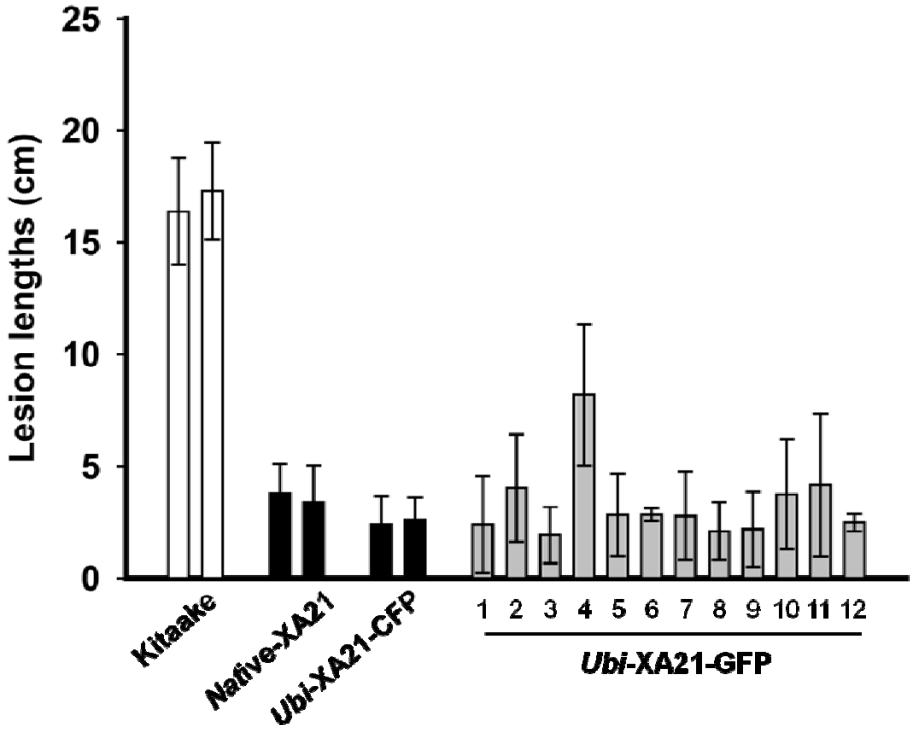

Supplementary Figure S5. Rice plants overexpressing *XA21-GFP* displayed enhanced resistance to *Xoo*.

Kitaake rice plants carrying *XA21* under the control of its native promoter (*Native*-XA21) (progeny from homozygous 23A-1-14)[18], rice plants carrying *XA21-CFP* under the control of *Ubi* promoter (*Ubi*-XA21-CFP, T_2 progeny from 7B-4)[18], and rice plants carrying *XA21-GFP* under the control of *Ubi* promoter (*Ubi*-XA21-GFP, T_0) were inoculated at six weeks of age (9 to 10 leaf stage) and lesion lengths were measured twelve DAI. Each data point represents the average and standard deviation of at least four independent replicates.

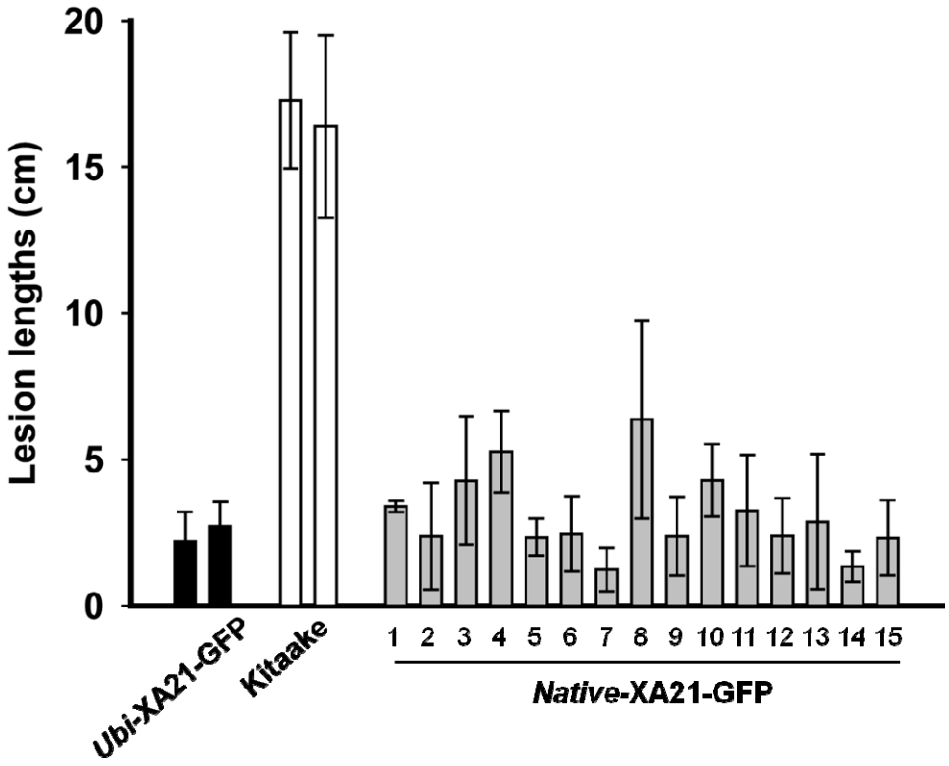

Supplementary Figure S6. Rice plants expressing *XA21-GFP* display enhanced resistance to *Xoo*.

Kitaake wild type, *Ubi*-XA21-GFP (T_1, 5-5), and Kitaake rice plants carrying *XA21-GFP* under the control of its native promoter (T_0, *Native*-XA21-GFP) were inoculated at six weeks of age (9 to 10 leaf stage). Lesion lengths were measured twelve DAI. Each data point represents the average and standard deviation of at least four independent replicates.

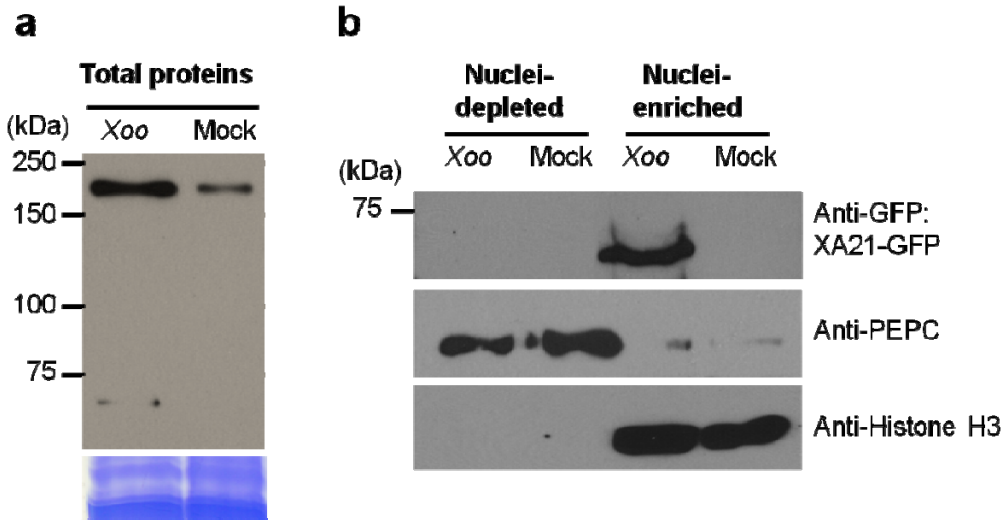

Supplementary Figure S7. Nuclear translocation of XA21-GFP after *Xoo* treatment.

(a) Western blot analysis of XA21-GFP proteins extracted from transgenic rice plants expressing *XA21-GFP* under the control of the native promoter (*Native*-XA21-GFP, 9-7). Equal amount of total proteins (120 μg) were extracted from leaf discs of Kitaake and *Native*-XA21-GFP plants three hours after *Xoo* treatment. XA21-GFP and C-terminal cleavage product, detected with an anti-GFP antibody, displayed bands of approximately 170 and 70 kDa, respectively. Equal loading of total proteins was confirmed by Coomassie blue staining of proteins (lower panel).

(b) Western blot analysis of XA21-GFP extracted from nuclei-depleted and nuclei-enriched fractions from *Native*-XA21-GFP line (9-7) detected by the anti-GFP antibody. Nuclei-enriched (150 μg) and nuclei-depleted (150 μg) fractions were prepared from total proteins in (a). XA21-GFP and C-terminal cleavage product-GFP displayed bands at approximately 170 and 70 kDa, respectively. Cytolsolic phosphoenolpyruvate carboxylase (PEPC) and nuclear histone H3 protein were used as cytosolic and nuclear markers, respectively.

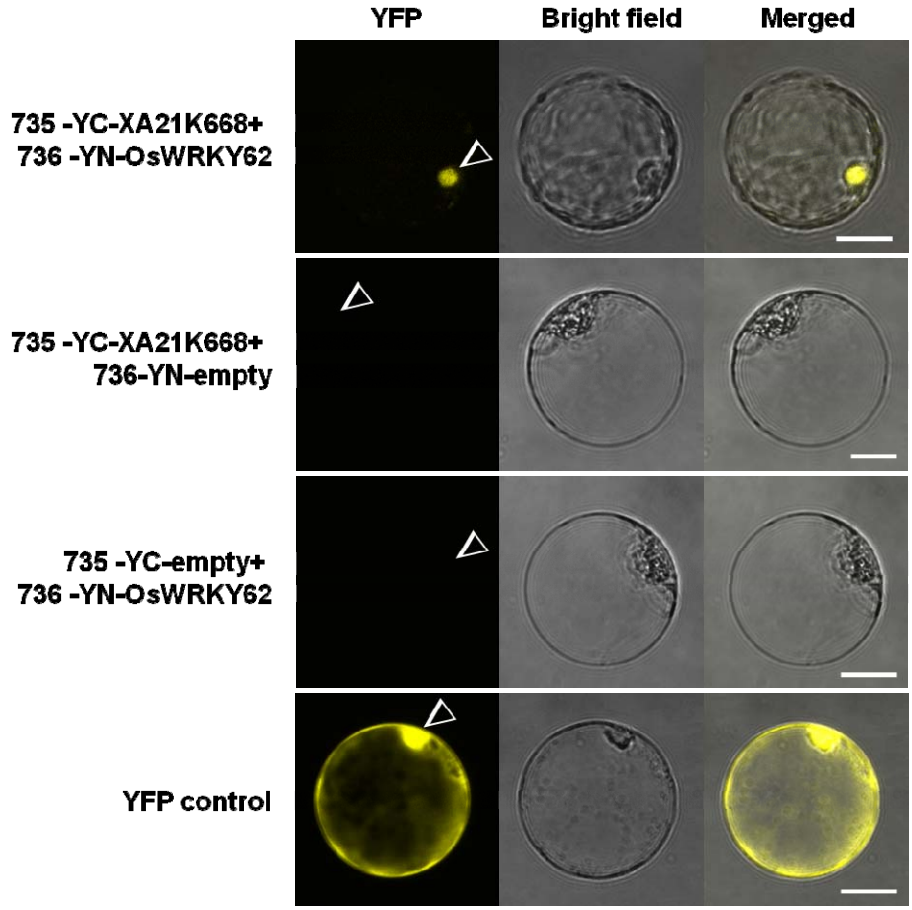

Supplementary Figure S8. XA21 interacts with OsWRKY62 in the nucleus.

Physical interaction between XA21K668 and OsWRKY62 was validated via bimolecular fluorescence complementation (BiFC). Shown are representative negative controls (735-YC-XA21K668 + 736-YN-empty and 735-YC-empty + 736-YN-OsWRKY62) and yellow fluorescent protein (YFP) control (*Ubi*-YFP). Images were taken 1 day after transformation. 735-YC and 736-YN indicate the gateway-converted vectors derived from pSY735 ($YFP_{C\text{-}term}$) and pSY736 ($YFP_{N\text{-}term}$) vector, respectively. Images were collected with a Leica True Confocal Scanner SPE confocal microscope and coded in yellow for YFP. Arrow heads mark the nuclei. Scale bar, 10 μm.

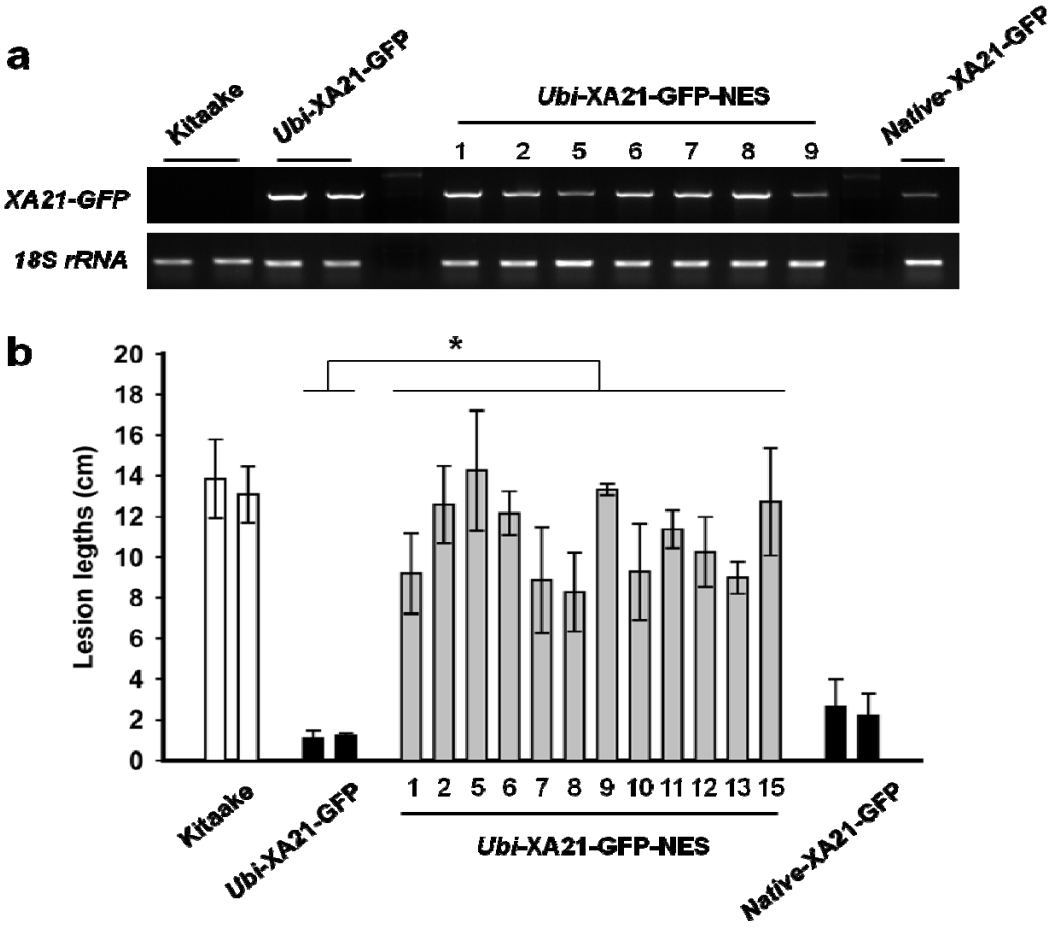

Supplementary Figure S9. Inhibition of nuclear translocation of XA21 compromised XA21-mediated immunity.

(a) *XA21-GFP-NES* transcripts significantly accumulated in *Ubi*-XA21-GFP-NES rice plants. Total RNA was extracted from six-week-old Kitaake wild type, *Ubi*-XA21-GFP (homozygous 5-5-4), *Ubi*-XA21-GFP-NES (T_0), and *Native*-XA21-GFP (T_1, 12-3). RT-PCR was performed with primers specific for *XA21-GFP*. Control RT-PCR reactions were carried out with *18S* rRNA.

(b) Kitaake wild type, *Ubi*-XA21-GFP (homozygous 5-5-4), *Ubi*-XA21-GFP-NES (T_0), and *Native*-XA21-GFP (T_1, 9-2 and 12-3) were inoculated at six-week-old age and lesion lengths were measured twelve DAI. Each data point represents the average and standard deviation of at least three samples. The asterisk (*) indicates statistically significant differences between each *Ubi*-XA21-GFP-NES and *Ubi*-XA21-GFP line (Student's *t*-tests, p value ≤ 0.05).

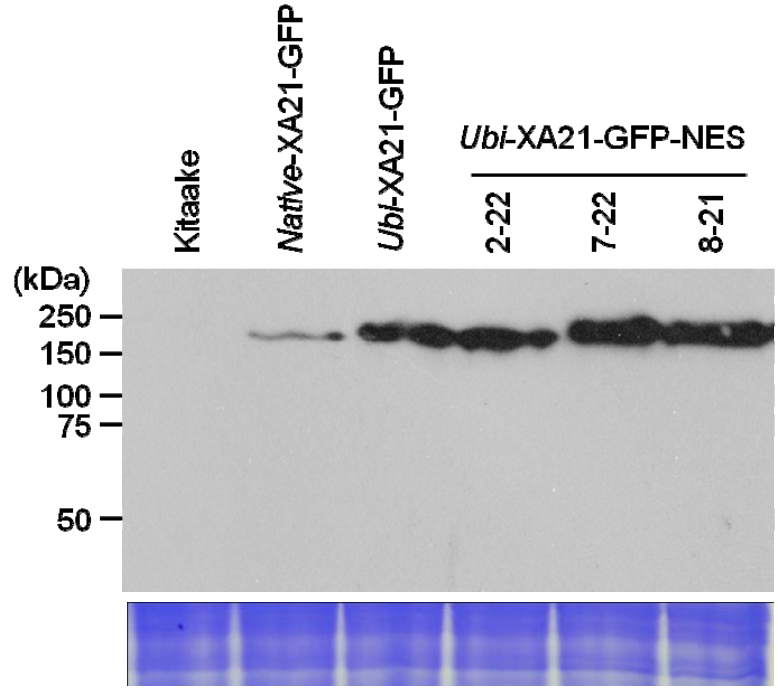

Supplementary Figure S10 The addition of a nuclear export signal (NES) does not affect the stability of the XA21-GFP protein.

Transgenic lines 2, 7, and 8 displayed a Mendelian segregation ratio (1:2:1), indicative of a single insertion of the transgene, *Ubi-XA21-GFP-NES*, into the genome (data not shown). Protein accumulation of the XA21-GFP-NES in transgenic lines, 2-22, 7-22, and 8-21 was compared with XA21-GFP in *Ubi*-XA21-GFP line. Equal amounts (100 μg) of total protein form *Ubi*-XA21-GFP (homozygous 5-5-4), *Ubi*-XA21-GFP-NES, and *Native*-XA21-GFP (T_1, 9-7) were extracted, analyzed by SDS-PAGE, and immunoblotted with anti-GFP antibody.

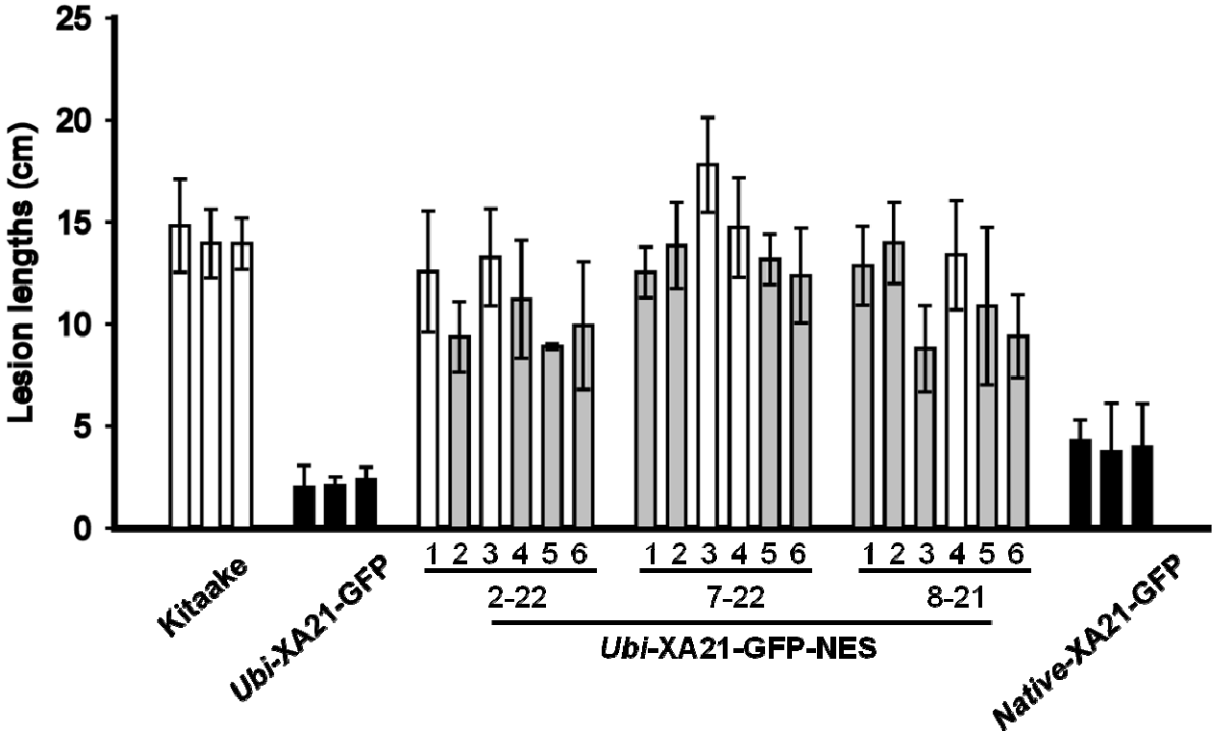

Supplementary Figure S11. Rice plants overexpressing *XA21-GFP-NES* are compromised in XA21-mediated immunity.

Kitaake, *Ubi*-XA21-GFP (homozygous 5-5-4), *Ubi*-XA21-GFP-NES (2-22, 7-22, and 8-21), and *Native*-XA21-GFP (T_2 progeny from 9-7) were inoculated at six weeks of age and lesion lengths were measured twelve DAI. Each data point represents the average and standard deviation of at least four independent replicates. Gray bars in *Ubi*-XA21-GFP-NES represent segregants carrying the transgene. White bars represent segregants not carrying the transgene.

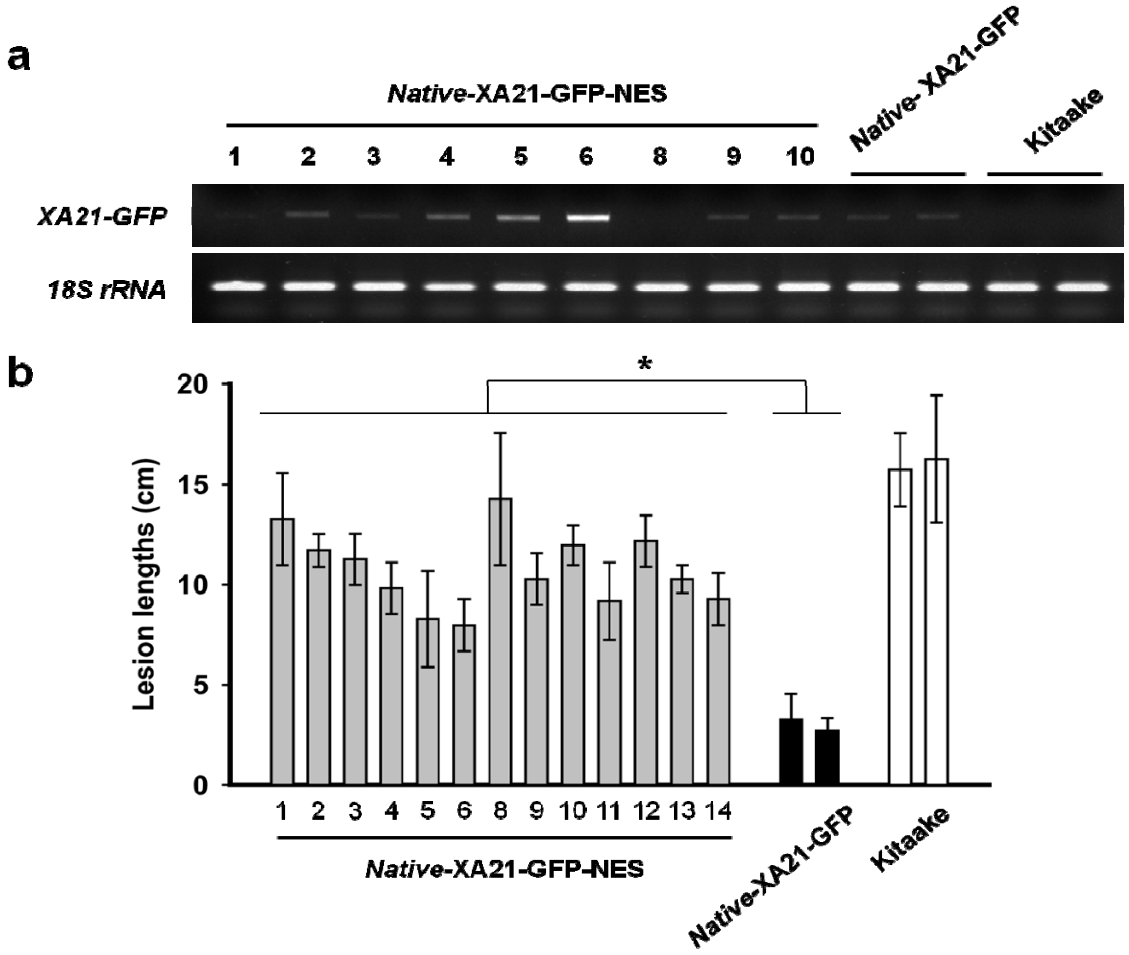

Supplementary Figure S12. Rice plants expressing *XA21-GFP-NES* are compromised in XA21-mediated immunity.

(a) *XA21-GFP-NES* transcript was expressed in the *Native*-XA21-GFP-NES rice plants. Total RNA was extracted from six-week-old Kitaake wild type, *Native*-XA21-GFP (T_2, 12-21 and 22), and *Native*-XA21-GFP-NES (T_0). RT-PCR was performed with primers specific for *XA21-GFP*. Control RT-PCR reactions were carried out with *18S* rRNA.

(b) Kitaake wild type, *Native*-XA21-GFP (T_2, 12-21 and 22), and *Native*-XA21-GFP-NES (T_0) were inoculated at six-week-old age and lesion lengths were measured twelve DAI. Each data point represents the average and standard deviation of at least five independent replicates. The asterisk (*) indicates statistically significant differences between each *Ubi*-XA21-GFP-NES and *Ubi*-XA21-GFP line (Student's *t*-tests, p value ≤ 0.05).

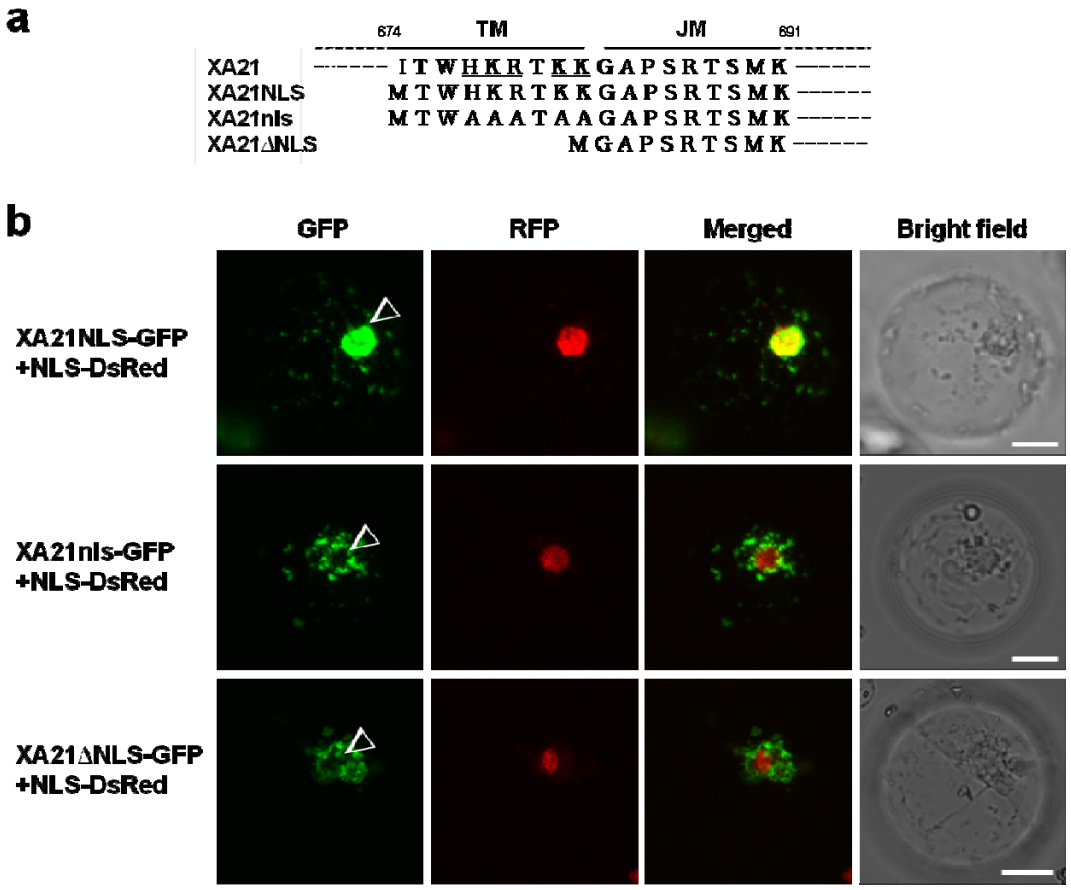

Supplementary Figure S13. XA21 carries a nuclear localization sequence.

(a) Schematic diagram of the region between the XA21 transmembrane (TM) and juxtamembrane (JM) domains. The basic amino acids in the putative XA21 nuclear localization sequence (NLS) are underlined. *XA21NLS* carries the XA21 intracellular domain and the putative NLS. The basic amino acids (H^{677}, K^{678}, R^{679}, K^{681}, and K^{682}) in the putative NLS are either mutated to alanines in the *XA21nls* construct or deleted in the *XA21ΔNLS* construct. TM, transmembrane domain; JM, juxtamembrane domain.

(b) The *XA21NLS-GFP*, *XA21nls-GFP*, and *XA21ΔNLS-GFP* variants were introduced into rice protoplast cells by PEG-mediated transformation. *NLS-DsRed* was co-transformed to serve as a nuclear marker. Images were collected with a Leica True Confocal Scanner SPE confocal microscope and coded in green or red for GFP and DsRed, respectively. Arrow heads mark the nuclei. Scale bar, 10 μm.

Supplementary Table S1. Quantification of XA21 localization change after Mock (non-treated), $AxY^{S}22$, and AxY22 treatment.

	Non-treated	$+AxY^{S}22$	+AxY22
XA21-GFP	1.2 ± 0.1*	24.1 ± 3.8	1.8 ± 0.7
XA21-GFP-NES	0.7 ± 0.6	0.9 ± 1.6	1.2 ± 0.2

*percentage of protoplasts showing signal from the nucleus

The *Ubi-XA21-GFP* and *Ubi-Xa21-GFP-NES* were introduced into rice protoplasts by PEG-mediated transformation. $AxY^{S}22$ or AxY22 peptide was applied 16 hours after transformation and XA21 localization change was observed one hour after peptide treatment. We scored the location of XA21-GFP in 70-90 protoplasts for each experiment. After cells expressing XA21-GFP or XA21-GFP-NES were counted, the percentage of protoplasts with 'nuclear expression' (strong nuclear signal as compared to the perinuclear region) was calculated[43].

Supplementary Reference

43 Asada, A. *et al.* Myristoylation of p39 and p35 is a determinant of cytoplasmic or nuclear localization of active cyclin-dependent kinase 5 complexes. *J. Neurochem.* **106**, 1325-1336 (2008).